Parquet approach to nonlocal vertex functions and electrical conductivity of disordered electrons

V. Janiš*
Institute of Physics, Academy of Sciences of the Czech Republic, Na Slovance 2, CZ-18221 Praha 8, Czech Republic
(Received 6 November 2000; published 31 August 2001)

A diagrammatic technique for two-particle vertex functions is used to describe systematically the influence of spatial quantum coherence and backscattering effects on transport properties of noninteracting electrons in a random potential. In analogy with many-body theory we construct parquet equations for topologically distinct *nonlocal* irreducible vertex functions into which the *local* one-particle propagator and two-particle vertex of the coherent-potential approximation (CPA) enter as input. To complete the two-particle parquet equations we use an integral form of the Ward identity and determine the one-particle self-energy from the known irreducible vertex. In this way a conserving approximation with (Herglotz) analytic averaged Green functions is obtained. We use the limit of high spatial dimensions to demonstrate how nonlocal corrections to the $d=\infty$ (CPA) solution emerge. The general parquet construction is applied to the calculation of vertex corrections to the electrical conductivity. With the aid of the high-dimensional asymptotics of the nonlocal irreducible vertex in the electron-hole scattering channel we derive a mean-field approximation for the conductivity with vertex corrections. The impact of vertex corrections onto the electronic transport is assessed quantitatively within the proposed mean-field description on a binary alloy.

DOI: 10.1103/PhysRevB.64.115115 PACS number(s): 71.23.An, 72.15.Eb, 72.15.Qm

I. INTRODUCTION

Randomness in the chemical composition or due to defects in solids causes elastic scatterings of charge carriers that influence significantly their motion and reduce their mobility. To describe the effects of randomly distributed scatterers reliably one has to use approximations taking satisfactorily into account quantum coherence between scattering events. In particular, self-consistence between one- and two-particle functions is needed if we want to assess the role of backscatterings and the backflow on transport properties of electrons in a random potential.

A simplest possibility to account for quantum coherence is to sum all multiple scatterings on a single scatterer. A self-consistent theory with all single-site scatterings is the coherent-potential approximation (CPA), which was developed in the end of the 1960s.[1,2] It is a mean-field approximation for disordered (noninteracting) electrons. It provides a local coherent potential (self-energy) that, in the thermodynamic limit, comprises the effects of the random potential on the motion of the single electron. The CPA, as other mean-field theories, however, suppresses spatial coherence between distinct scattering centers and the moving electrons feel the influence of the random potential only via an averaged medium.

CPA has proven very successful in the description of one-electron properties at the model level as well as in realistic calculations of random alloys.[3,4] Although this approximation can as well describe two-particle averaged functions, due to the lack of spatial coherence, it fails to capture backscattering effects on the transport coefficients and the electrical conductivity. The two-particle CPA vertex does not depend on the transfer momentum between the incoming and the outgoing particles and hence the CPA conductivity reduces in the single-band bulk systems to a contribution from a single particle-hole bubble. There are no vertex corrections to the electrical conductivity within the standard single-band CPA.[5]

Vertex corrections to the single-bubble one-electron conductivity are important in various situations. In low dimensions ($d\leqslant 2$) or for sufficiently strong disorder they lead to Anderson localization.[6] Further on, tunnel conductance or transport through multilayered dirty metals are essentially influenced by vertex corrections.[7] To obtain more realistic results for the electronic transport in dirty metals one has to go beyond the standard CPA to the conductivity and develop approximations containing spatial quantum coherence and backscattering contributions.

There is a long history of efforts to improve upon the mean-field CPA description of disordered electrons.[8] Most of them concentrate on single-particle properties and improve upon the CPA in the self-energy (coherent potential). A natural extension of the single-site theory is to use clusters self-consistently embedded in an averaged medium. However, apart from the traveling-cluster approximation,[9,10] extensions in the lattice space fail to warrant global analytic properties of the solution and hence spurious effects can emerge.[11,12] Only recently a cluster expansion in momentum space was suggested that warrants analytic (Herglotz) properties of the resulting averaged propagators and the self-energy at each stage.[13] Cluster approximations with self-energy diagrams improve also two-particle vertex functions. However, cluster approximations reduce spatial quantum coherence only to a discrete set of lattice sites or momenta. Such approximations then remain perturbative in the coherence range and cannot lead to Anderson localization to which we need long-range coherence with infinite-many backscattering or ''crossed'' diagrams.[14,15]

Using cluster approximations to improve upon the mean-field transport properties means that we have first to extend the one-electron calculation scheme. A tremendous effort at the one-particle level is to be exerted to obtain significant changes in transport properties. Cluster expansions are hence not very effective in calculating quantum coherence effects in the electrical conductivity. It is more efficient to develop

approximations directly for two-particle functions.

A suitable framework for developing two-particle approximations is a parquet approach devised within quantum many-body theory.[16–19] It is an advanced scheme of summation of Feynman (many-body) diagrams based on renormalizations of two-particle vertex functions. Its main idea is to utilize ambiguity in the definition of the two-particle irreducibility. Each two-particle irreducibility, i.e., the way pairs of one-particle propagators are cut without disconnecting the diagram, defines a scattering channel and a Bethe-Salpeter equation for the full two-particle vertex. Since different two-particle channels are topologically inequivalent, a solution of the Bethe-Salpeter equation from one channel (reducible function) is irreducible in the other channels where it is used in the input (integral kernel) in the respective Bethe-Salpeter equations. Thereby a set of coupled, nonlinear self-consistent equations for the two-particle irreducible vertices (parquet equations) is obtained. Parquet equations have been applied onto various many-body problems, but no significant attempt has been made to use the parquet-type renormalization of Feynman diagrams in disordered systems.

In this paper we develop a parquet approach to systems with noninteracting electrons subjected to a random potential. We show how to construct controlled approximations directly for the two-particle vertex using the idea of parquet diagrams. Since the parquet construction applies only to nonlocal propagators, we start from the limit of high spatial dimensions where the diagonal and off-diagonal one-particle propagators separate and the CPA becomes exact.[21] Beyond this limit we construct parquet equations for two-particle irreducible vertices from Bethe-Salpeter equations with a perturbed nonlocal one-particle propagator and the local two-particle vertex as input. Next we use a Ward identity to determine the self-energy and the full one-particle averaged propagator from the calculated vertex functions. This self-consistent procedure warrants conservation laws and analytic properties of the one-particle functions whenever the solutions to the two-particle parquet equations are analytic.

The unrestricted system of parquet equations is not soluble in general. We hence resort to high spatial dimensions where the two-particle self-consistence is naturally suppressed and one obtains the asymptotic form of the two-particle vertex in closed form.[22,20] We use this explicit result to derive a mean-field approximation for the electrical conductivity containing vertex corrections. We then choose a binary alloy to make quantitative assessments of the impact of vertex corrections on the bulk conductivity.

The paper is organized as follows. We derive in Sec. II the parquet equations for vertex functions of disordered electrons. In Sec. III we show how Ward identities can be used to determine the self-energy from a given irreducible vertex function so that we preserve conserving character of the approximation. The electrical conductivity with the irreducible vertex function in the electron-hole scattering channel is derived in Sec. IV where we use the result to construct a mean-field approximation for the electrical conductivity with vertex corrections. In Sec. V we first quantitatively assess the mean-field approximation with vertex corrections on an example of a binary alloy in high spatial dimensions. Then the reliability of mean-field approximations in realistic calculations of bulk transport properties of metallic alloys is briefly discussed.

II. CALCULATION OF THE VERTEX FUNCTION

We use a tight-binding Anderson model of noninteracting spinless electrons moving in a random, site-diagonal potential V_i described by a Hamiltonian

$$\hat{H}_{AD}=\sum_{\langle ij\rangle} t_{ij}c_i^\dagger c_j+\sum_i V_i c_i^\dagger c_i . \tag{1}$$

The values of the random potential V_i are site independent and obey a disorder distribution $\rho(V)$. I.e., a function depending on the random potential V_i is averaged via

$$\langle X(V_i)\rangle_{av}=\int_{-\infty}^{\infty} dV\rho(V)X(V). \tag{2}$$

Solving the problem of disordered electrons in thermodynamic equilibrium amounts to finding the averaged free energy defined as

$$F_{av}=-k_BT\langle \ln \mathrm{Tr}\exp\{-\beta\hat{H}_{AD}(t_{ij},V_i)\}\rangle_{av}, \tag{3}$$

where the trace Tr runs over the electronic degrees of freedom in the Fock space. However, the averaged free energy does not contain the entire information about the disordered system. In particular we cannot derive transport properties and the response to disturbing external forces from it. We need to know averaged products of Green functions for different energies. To include external perturbations into the thermodynamic description we introduce a new quantity $\Omega^\nu(E_1,E_2,\ldots,E_\nu;U)$. It is a generalized averaged grand potential with ν energy states coupled via an external perturbation U. We define

$$\begin{aligned}\Omega^\nu(E_1,E_2,\ldots,E_\nu;U)&\\ =-k_BT\Bigg\langle \ln \mathrm{Tr}\exp\Bigg\{-\beta\sum_{i,j=1}^{\nu}&(\hat{H}_{AD}^{(i)}\delta_{ij}\\ -E_i\hat{N}^{(i)}\delta_{ij}+\Delta\hat{H}^{(ij)})\Bigg\}\Bigg\rangle_{av},&\end{aligned} \tag{4}$$

where we assigned to each (complex) energy E_i a separate Hilbert state space and $\Delta\hat{H}^{(ij)}=\Sigma_{kl}U_{kl}^{(ij)}c_k^{(i)\dagger}c_l^{(j)}$. Potential $\Omega^\nu(E_1,E_2,E_\nu;U)$ is a generating functional for averaged products of Green functions up to the νth order. In practice, within linear-response theory we will use only one- and two-particle Green functions, i.e., $\Omega^\nu(E_1,E_2,\ldots,E_\nu;U)$ is expanded up to U^2.

Averaged Green functions (propagators) are fundamental quantities with the aid of which we can calculate all characteristics of the disordered system. We can use momenta as good quantum numbers, since translational invariance is restored for the averaged quantities. Averaged propagators can

then be expressed as sums of Feynman diagrams for disordered systems in analogy to the standard many-body diagrams.[23]

The averaged one-particle propagator is represented with the aid of the self-energy or a coherent potential $\Sigma(\mathbf{k},z)$ that comprises the influence of fluctuations of the random potential onto the motion of the single electron. We write

$$G(\mathbf{k},z)=\frac{1}{z-\epsilon(\mathbf{k})-\Sigma(\mathbf{k},z)}$$
$$=\frac{1}{N}\sum_{ij} e^{-i\mathbf{k}(\mathbf{R}_i-\mathbf{R}_j)}\langle[z\hat{1}-\hat{t}-\hat{V}]^{-1}_{ij}\rangle_{av}, \quad (5)$$

where the first equality expresses the Dyson equation connecting the irreducible one-particle function (self-energy) with the one-particle averaged propagator.

The averaged two-particle propagator is defined as

$$G^{(2)}_{ij,kl}(z_1,z_2)=\langle[z_1\hat{1}-\hat{t}-\hat{V}]^{-1}_{ij}[z_2\hat{1}-\hat{t}-\hat{V}]^{-1}_{kl}\rangle_{av} \quad (6)$$

to which we define the Fourier transform to momentum space as follows:

$$G^{(2)}(\mathbf{k}_1,z_1,\mathbf{k}_2,z_2;\mathbf{q})=\frac{1}{N}\sum_{ijkl} e^{-i\mathbf{k}_1\mathbf{R}_i}e^{i(\mathbf{k}_1+\mathbf{q})\mathbf{R}_j}$$
$$\times e^{-i(\mathbf{k}_2+\mathbf{q})\mathbf{R}_k}e^{i\mathbf{k}_2\mathbf{R}_l}G^{(2)}_{ij,kl}(z_1,z_2). \quad (7)$$

The two-particle Green function $G^{(2)}(\mathbf{k}_1,z_1,\mathbf{k}_2,z_2;\mathbf{q})$ contains also uncorrelated motion of two separate particles. The actual measure of a correlated motion of two particles is a vertex function

$$\Gamma(\mathbf{k}_1,z_1,\mathbf{k}_2,z_2;\mathbf{q})$$
$$=G^{-1}(\mathbf{k}_1,z_1)G^{-1}(\mathbf{k}_2,z_2)[G^{(2)}(\mathbf{k}_1,z_1,\mathbf{k}_2,z_2;\mathbf{q})-\delta(\mathbf{q})$$
$$\times G(\mathbf{k}_1,z_1)G(\mathbf{k}_2,z_2)]G^{-1}(\mathbf{k}_1+\mathbf{q},z_1)G^{-1}(\mathbf{k}_2+\mathbf{q},z_2). \quad (8)$$

In analogy to the Dyson equation for the one-particle propagator we can represent the two-particle vertex with the aid of a two-particle irreducible vertex Λ and a Bethe-Salpeter equation. Unlike the one-particle case, the Bethe-Salpeter equation is not defined unambiguously whenever we work with nonlocal propagators. This fact we utilize later in the parquet construction. For the present moment we take the Bethe-Salpeter equation in the electron-hole channel describing multiple scatterings of a pair of an electron and a hole and write

$$\Gamma(\mathbf{k}_1,z_1,\mathbf{k}_2,z_2;\mathbf{q})$$
$$=\Lambda(\mathbf{k}_1,z_1,\mathbf{k}_2,z_2;\mathbf{q})+\frac{1}{N}\sum_{\mathbf{q}''}\Lambda(\mathbf{k}_1,z_1,\mathbf{k}_2,z_2;\mathbf{q}'')$$
$$\times G(\mathbf{k}_1+\mathbf{q}'',z_1)G(\mathbf{k}_2+\mathbf{q}'',z_2)\Gamma(\mathbf{k}_1+\mathbf{q}'',z_1,$$
$$\mathbf{k}_2+\mathbf{q}'',z_2;\mathbf{q}-\mathbf{q}''). \quad (9)$$

The one- and two-particle irreducible functions, i.e., self-energy $\Sigma(\mathbf{k},z)$ and vertex $\Lambda(\mathbf{k}_1,z_1,\mathbf{k}_2,z_2;\mathbf{q})$ are the quantities that we have to approximate in order to determine the one- and two-particle characteristics of a disordered system. The two functions are not completely independent. In a conserving and thermodynamically consistent approximation we have a generalized differential Ward identity[24]

$$\Lambda(\mathbf{k}_1,z_1,\mathbf{k}_2,z_2;\mathbf{q})=\left.\frac{\delta\Sigma(\mathbf{k}_1,z_1,\mathbf{k}_2,z_2;U)}{\delta G(\mathbf{k}_1+\mathbf{q},z_1,\mathbf{k}_2+\mathbf{q},z_2;U)}\right|_{U=0}. \quad (10)$$

We could use it for the determination of the irreducible vertex if we knew explicitly the self-energy as a functional of the averaged propagator in the presence of the external disturbance U. It is rarely the case. We, however, show in Sec. III how to use an integral form of the Ward identity to determine the self-energy from the known irreducible vertex Λ. It is then sufficient to construct an approximation for the two-particle irreducible vertex Λ, which will be done in the following subsections.

A. Local approximation

We start building approximations to the two-particle vertex function from a local solution where we completely lose momentum dependence. The local approximation means that we use only site-diagonal one-particle propagators in the perturbation diagrammatic expansion for the irreducible functions. The local approximation is best derived within the Baym-Kadanoff renormalized perturbation expansion in the limit of high spatial dimensions $d\to\infty$.[22] In this limit we have the following asymptotics for the one-particle functions:

$$G=G^{diag}[d^0]+G^{off}[d^{-1/2}], \quad \Sigma=\Sigma^{diag}[d^0]+\Sigma^{off}[d^{-3/2}] \quad (11)$$

leading to separation of the diagonal (local) and the off-diagonal (nonlocal) parts. In the strict limit $d=\infty$ we can completely neglect the off-diagonal elements and recover the CPA for the self-energy. The defining equation in the presence of the external local disturbance U reads

$$\hat{G}(z_1,z_2;U)=\langle[\hat{G}^{-1}(z_1,z_2;U)+\hat{\Sigma}(z_1,z_2;U)-\hat{V}_i]^{-1}\rangle_{av}, \quad (12)$$

where $\hat{G}(z_1,z_2;U)=N^{-2}\Sigma_{\mathbf{k}_1\mathbf{k}_2}\hat{G}(\mathbf{k}_1,z_1,\mathbf{k}_2,z_2;U)$ is the local element of the matrix one-particle propagator. The matrix character is forced by the external disturbance which mixes different complex energies. Since we are interested only in averaged two-particle functions in equilibrium, we can resort to two energies and a two-by-two matrix

$$\hat{G}^{-1}(\mathbf{k}_1,z_1,\mathbf{k}_2,z_2;U) = \begin{pmatrix} z_1-\epsilon(\mathbf{k}_1)-\Sigma(z_1) & U-\Sigma(z_1,z_2;U) \\ U-\Sigma(z_2,z_1;U) & z_2-\epsilon(\mathbf{k}_2)-\Sigma(z_2) \end{pmatrix}, \tag{13}$$

where $\epsilon(\mathbf{k})$ is the lattice dispersion relation.

We use the Ward identity (10) to determine the two-particle irreducible vertex in equilibrium

$$\Lambda(z_1,z_2)=\left.\frac{\delta\Sigma_U(z_1,z_2)}{\delta G_U(z_1,z_2)}\right|_{U=0} = \frac{1}{G(z_1)G(z_2)}\left[1-\left\langle \frac{1}{1+(\Sigma(z_1)-V_i)G(z_1)} \times \frac{1}{1+(\Sigma(z_2)-V_i)G(z_2)}\right\rangle_{av}^{-1}\right]. \tag{14}$$

The full vertex function is then determined from the Bethe-Salpeter Eq. (9) where the one-particle propagators are replaced with the local ones. The integral equation reduces to an algebraic one and we obtain an explicit representation

$$\gamma(z_1,z_2)=\frac{\Lambda(z_1,z_2)}{1-\Lambda(z_1,z_2)G(z_1)G(z_2)}. \tag{15}$$

For later convenience we denoted the full local two-particle vertex with the lower case γ.

Note that the above local approximation coincides with the CPA only for the self-energy and the local part of the vertex function. The CPA two-particle vertex is obtained from Eq. (9) where only the irreducible vertex $\Lambda(z_1,z_2)$ is assumed local, but not the one-particle propagators.[5] Here we deliberately separated the contribution from the off-diagonal propagator. We describe it within the parquet approach as a correction to the local approximation to the vertex function.

B. Nonlocal contributions: Parquet approach

To go beyond the local approximation we have to distinguish two one-particle propagators. First, we have the propagator from the local approximation that we denote $G^{loc}(\mathbf{k},z)$, from which we actually need only the local element $G^{loc}(z)=N^{-1}\Sigma_{\mathbf{k}}G^{loc}(\mathbf{k},z)$. This propagator is defined by the Dyson equation with the local self-energy $\Sigma(z)$ from Eq. (12) with $U=0$. Second, we have to introduce a new propagator $G(\mathbf{k},z)$ that is defined by the Dyson equation with a nonlocal self-energy $\Sigma(\mathbf{k},z)$ to be determined later. It is treated in the equations for the two-particle vertex as an external function with appropriate analytic properties. In the expansion beyond the local approximation we use a perturbed propagator $\tilde{G}(\mathbf{k},z)=G(\mathbf{k},z)-G^{loc}(z)$ to avoid multiple summations of single-site diagrams contained in the local approximation.

We classify *nonlocal* contributions to the two-particle vertex by the type of the correlated two-particle propagation. We either simultaneously propagate an electron and a hole or two electrons (holes). Diagrammatically it means that we connect *spatially distinct* two-particle scattering events with antiparallel or parallel pairs of one-particle propagators. Multiple scatterings of pairs of the same type define a channel of the two-particle irreducibility. We call a diagram two-particle irreducible if it cannot be split into separate parts by cutting simultaneously either electron-hole or electron-electron propagators. The two definitions of the two-particle irreducibility lead to topologically inequivalent irreducible functions and to different Bethe-Salpeter equations for the full vertex. In each Bethe-Salpeter equation the two-particle functions are interconnected via one-particle propagators in a different manner. We can generically represent the Bethe-Salpeter equations as

$$\Gamma(\mathbf{k}_1,z_1,\mathbf{k}_2,z_2;\mathbf{q})=\tilde{\Lambda}^{\alpha}(\mathbf{k}_1,z_1,\mathbf{k}_2,z_2;\mathbf{q}) + [\tilde{\Lambda}^{\alpha}\tilde{G}\tilde{G}\odot\Gamma](\mathbf{k}_1,z_1,\mathbf{k}_2,z_2;\mathbf{q}). \tag{16}$$

We used $\odot$ for the channel-dependent multiplication of the two-particle functions. Here $\tilde{\Lambda}^{\alpha}$ is the irreducible vertex in the α channel with perturbed propagators $\tilde{G}$. It relates to the standard irreducible vertex function Λ^{α} from Bethe-Salpeter equations with full one-particle propagators as follows:

$$\Lambda^{\alpha}(\mathbf{k}_1,z_1,\mathbf{k}_2,z_2;\mathbf{q}) = \tilde{\Lambda}^{\alpha}(\mathbf{k}_1,z_1,\mathbf{k}_2,z_2;\mathbf{q}) - [\tilde{\Lambda}^{\alpha}G^{loc}(z_1)G^{loc}(z_2)\odot\Lambda^{\alpha}](\mathbf{k}_1,z_1,\mathbf{k}_2,z_2;\mathbf{q}). \tag{17}$$

Although the irreducible functions are different in different channels the solution of the Bethe-Salpeter equations must always be the same, the full two-particle vertex Γ. The matrix multiplication in momentum space in the electron-hole and electron-electron channels, respectively, explicitly reads

$$[\hat{X}GG\bullet\hat{Y}](\mathbf{k}_1,z_1,\mathbf{k}_2,z_2;\mathbf{q}) = \frac{1}{N}\sum_{\mathbf{q}''} X(\mathbf{k}_1,z_1,\mathbf{k}_2,z_2;\mathbf{q}'')G(\mathbf{k}_1+\mathbf{q}'',z_1) \times G(\mathbf{k}_2+\mathbf{q}'',z_2)Y(\mathbf{k}_1+\mathbf{q}'',z_1,\mathbf{k}_2+\mathbf{q}'',z_2;\mathbf{q}-\mathbf{q}''), \tag{18a}$$

$$[\hat{X}GG\circ\hat{Y}](\mathbf{k}_1,z_1,\mathbf{k}_2,z_2;\mathbf{q}) = \frac{1}{N}\sum_{\mathbf{q}''} X(\mathbf{k}_1,z_1,\mathbf{k}_2+\mathbf{q}'',z_2;\mathbf{q}-\mathbf{q}'')G(\mathbf{k}_1+\mathbf{q}-\mathbf{q}'',z_1) \times G(\mathbf{k}_2+\mathbf{q}'',z_2)Y(\mathbf{k}_1+\mathbf{q}-\mathbf{q}'',z_1,\mathbf{k}_2,z_2;\mathbf{q}''). \tag{18b}$$

Electron-hole and electron-electron channels are not the only inequivalent representations of multiple two-particle scatterings. If we allow for hopping between distant sites we no longer can distinguish between multiple scatterings of distinct electron-hole pairs or nonlocal self-scatterings of a single particle, i.e., scatterings between the incoming and the

outgoing particles at the two-particle vertex. We hence have to introduce a third two-particle irreducibility and Bethe-Salpeter equation. We call this third type of two-particle scatterings ''vertical channel,'' since we renormalize only one line of the pair and the ladder of multiple scatterings grows ''vertically'' above (below) the two-particle vertex. We can write the third multiplication scheme for two-particle quantities for the upper particle line (with energy z_1)

$$[\hat{X}GG\star\hat{Y}](\mathbf{k}_1,z_1,\mathbf{k}_2,z_2;\mathbf{q})$$

$$=\frac{1}{N}\sum_{\mathbf{k}''}X(\mathbf{k}_1,z_1,\mathbf{k}_1+\mathbf{q},z_1;\mathbf{k}''-\mathbf{k}_1)G(\mathbf{k}'',z_1)$$

$$\times G(\mathbf{k}''+\mathbf{q},z_1)Y(\mathbf{k}'',z_1,\mathbf{k}_2,z_2;\mathbf{q}) \tag{18c}$$

and for the lower one (with energy z_2)

$$[\hat{X}\star GG\hat{Y}](\mathbf{k}_1,z_1,\mathbf{k}_2,z_2;\mathbf{q})$$

$$=\frac{1}{N}\sum_{\mathbf{k}''}X(\mathbf{k}_1,z_1,\mathbf{k}'',z_2;\mathbf{q})G(\mathbf{k}'',z_2)G(\mathbf{k}''+\mathbf{q},z_2)$$

$$\times Y(\mathbf{k}'',z_2,\mathbf{k}''+\mathbf{q},z_2;\mathbf{k}_2-\mathbf{k}''). \tag{18d}$$

In the vertical channel only one energy z_1 or z_2 is renormalized. The vertical channel hence splits into two, upper and lower parts according to whether we renormalize the first or the second energy in the pair.

Using the above multiplication schemes for different two-particle channels we can write down the corresponding Bethe-Salpeter equations explicitly. We choose a subscript $\alpha=\pm$ for complex half-planes from which we take the particle energy. We use the standard diagrammatic representation for these equations and obtain for the electron-hole and electron-electron channels

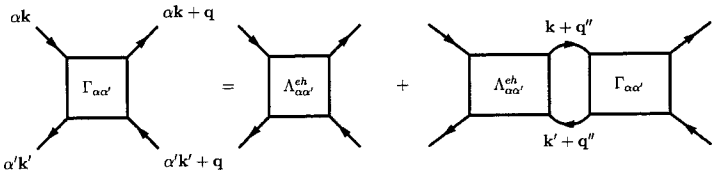

(19a)

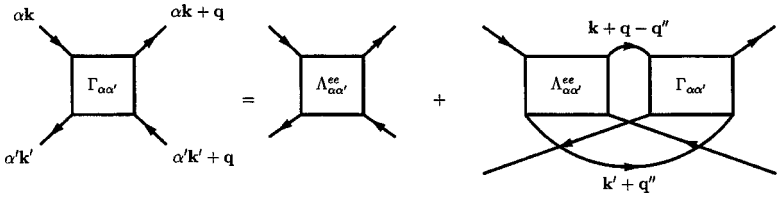

(19b)

The Bethe-Salpeter equation in the vertical channel is split into two. First we account for self-scattering vertex corrections to the upper line and then the same for the lower one. We then have

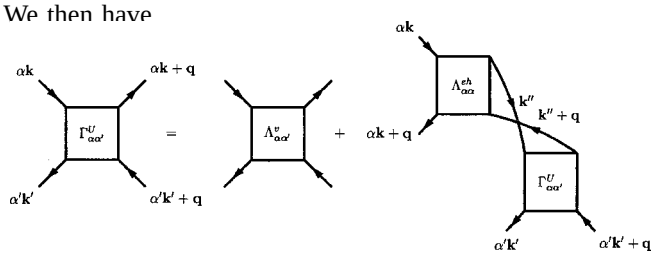

(19c)

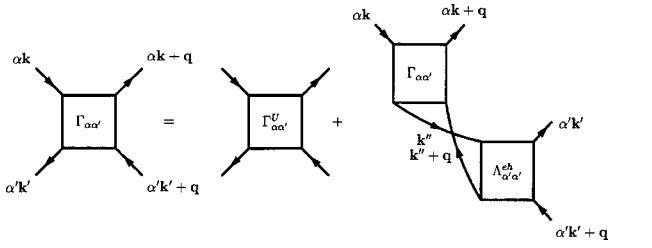

(19d)

Note that it is the irreducible vertex from the electron-hole channel Λ^{eh} that determines the kernel of the integral Eqs. (19c) and (19d). The new vertex Λ^{v} enters only via the absolute term. The irreducible vertices Λ^{v} and Λ^{eh} are not generally equal and it is useful for our construction to distinguish the vertical channel from the other two.

In all these equations the double-prime momenta are summed over. The full lines stand for the perturbed propagators $\tilde{G}(\mathbf{k},z)$. Otherwise we would encounter multiple summations of single-site scatterings. Separation of the local and nonlocal contributions is important, since in the local approximation the three channels coincide. This can be seen from Eq. (18) when we insert a local propagator. This fact is physically obvious, since we cannot distinguish between the particle and the hole in single-site multiple scatterings. The electron and the hole propagators are equal. There is only one two-particle irreducible vertex $\Lambda(z_1,z_2)$ in the local approximation (CPA).

We now use the topological inequivalence of the three channels. This means that a reducible function from one channel is irreducible in the other ones. If we denote I the completely irreducible two-particle vertex[25] we can write

$$\tilde{\Lambda}^{\alpha}(\mathbf{k}_1,z_1,\mathbf{k}_2,z_2;\mathbf{q}) = I(\mathbf{k}_1,z_1,\mathbf{k}_2,z_2;\mathbf{q}) + \sum_{\alpha'\neq\alpha} (\Gamma(\mathbf{k}_1,z_1,\mathbf{k}_2,z_2;\mathbf{q}) - \tilde{\Lambda}^{\alpha'}(\mathbf{k}_1,z_1,\mathbf{k}_2,z_2;\mathbf{q})), \tag{20a}$$

since the reducible function is a difference between the full and the irreducible vertex from a given channel. We use the Bethe-Salpeter Eqs. (19) on the right-hand side of Eq. (20a) from the corresponding α' channel to get rid of the full vertex. We then obtain a set of equations for the channel-dependent irreducible vertices $\tilde{\Lambda}^{\alpha}$. The completely irreducible vertex is input to these so-called parquet equations. The lowest-order contribution to the input function is the local two-particle vertex γ. The parquet equations in a generic form are

$$\tilde{\Lambda}^{\alpha}(\mathbf{k}_1,z_1,\mathbf{k}_2,z_2;\mathbf{q}) = \gamma(z_1,z_2) + \sum_{\alpha'\neq\alpha} \{1-[\tilde{\Lambda}^{\alpha'}\tilde{G}\tilde{G}]\odot\}^{-1} \times [\tilde{\Lambda}^{\alpha'}\tilde{G}\tilde{G}\odot\tilde{\Lambda}^{\alpha'}](\mathbf{k}_1,z_1,\mathbf{k}_2,z_2;\mathbf{q}). \tag{20b}$$

Special attention should be paid to the vertical channel, $\alpha'=v$, where we have a two-step construction and Bethe-Salpeter Eqs. (19c) and (19d). The second term on the right-hand side of Eq. (20b) should be replaced by $\{1-[\tilde{\Lambda}^{eh}\tilde{G}\tilde{G}]\star\}^{-1}\tilde{\Lambda}^{v}\{1-\star[\tilde{G}\tilde{G}\tilde{\Lambda}^{eh}]\}^{-1}-\tilde{\Lambda}^{v}$.

Equations (20) constitute the parquet approximation for the irreducible vertices for the given one-particle propagators $G(\mathbf{k},z)$, $G^{loc}(z)$ and the local two-particle vertex $\gamma(z_1,z_2)$, that again is a function of G^{loc} from Eq. (15). The latter propagator is determined from the local approximation, CPA. The former is treated here as a function of a self-energy $\Sigma(\mathbf{k},z)$ which we connect to the vertex functions later on. Parquet Eqs. (20b) form a set of nonlinear integral equations self-consistently determining the two-particle irreducible vertex functions $\Lambda^{\alpha}[\Sigma;G^{loc}]$.

The parquet equations represent a substantial extension of the local approximation. They are, however, much more difficult to solve than cluster or other short-range extensions of the CPA at the one-particle level. To get a feeling of how a solution to the parquet equations looks we resort to the asymptotic limit $d\to\infty$ where the corrections to the local vertex $\gamma(z_1,z_2)$ in Eq. (20b) asymptotically vanish.[22] The two-particle self-consistence becomes asymptotically insignificant and such a situation can be dealt with exactly.

C. Asymptotic limit of high spatial dimensions

We know that the off-diagonal, nonlocal elements are scaled to zero in high dimensions and loose their weight with respect to the local ones.[26] However, when summed over the lattice sites they can produce finite contributions even in the limit $d=\infty$. It is the case of the two-particle vertex. In the leading asymptotic order the irreducible vertices in the Bethe-Salpeter equations become local and coincide with $\gamma(z_1,z_2)$. The asymptotic behavior of the full vertex then depends upon which matrix element we calculate. We obtain different asymptotic solutions in different channels that we denote Γ^{α}.[22] The corresponding asymptotic Bethe-Salpeter equations in the three channels have the following diagrammatic representation

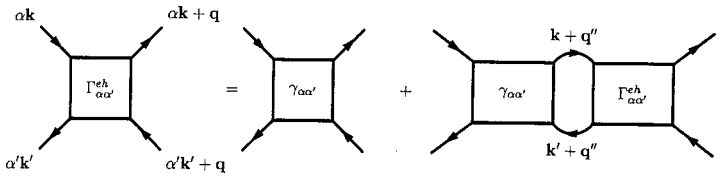

(21a)

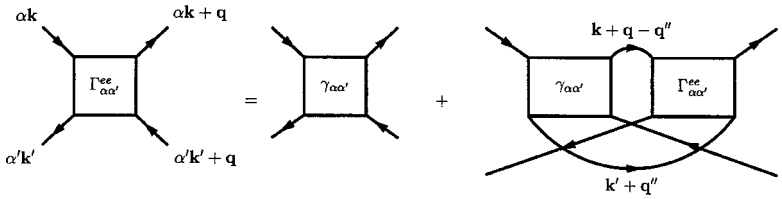

(21b)

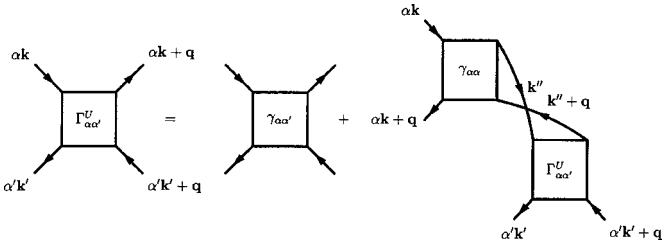

(21c)

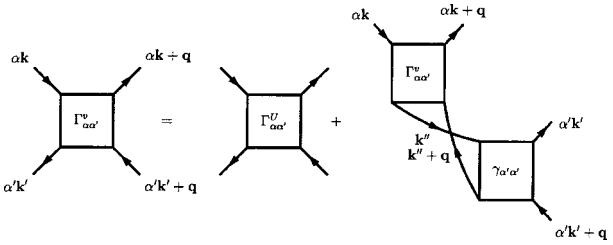

“

(21d)

The one-particle propagator in the high-dimensional Bethe-Salpeter equations equals the CPA solution, $G(\mathbf{k},z)=G^{loc}(\mathbf{k},z)$, or $\Sigma(\mathbf{k},z)=\Sigma^{CPA}(z)$. We sum over the intermediate momenta in the Bethe-Salpeter equations. The nonlocal part of $G^{loc}(\mathbf{k},z)$ cannot be neglected and contributes to the leading asymptotic behavior of the solution for fixed two-particle momenta.

The Bethe-Salpeter equations (21) in high dimensions become algebraic and can be solved in closed form. If we denote

$$Y^{\pm}(\mathbf{q};z_1,z_2)=\frac{1}{N}\sum_{\mathbf{k}} G^{off}(\mathbf{k},z_1)G^{off}(\mathbf{q}\pm\mathbf{k},z_2), \quad (22)$$

the solutions in the three channels are

$$\Gamma^{eh}(\mathbf{q};z_1,z_2)=\frac{\gamma(z_1,z_2)}{1-\gamma(z_1,z_2)Y^{+}(\mathbf{q};z_1,z_2)}, \quad (23a)$$

$$\Gamma^{ee}(\mathbf{q};z_1,z_2)=\frac{\gamma(z_1,z_2)}{1-\gamma(z_1,z_2)Y^{-}(\mathbf{q};z_1,z_2)} \quad (23b)$$

$$\Gamma^{v}(\mathbf{q};z_1,z_2)=\gamma(z_1,z_2)\prod_{i=1}^{2}\frac{1}{[1-\gamma(z_i,z_i)Y^{+}(\mathbf{q};z_i,z_i)]}. \quad (23c)$$

The three different vertex functions represent the three asymptotic solutions we obtain in the limit of high spatial dimensions. Each solution is characterized by a two-particle conserved momentum. They are in the notation from the preceding subsection $\mathbf{k}_1-\mathbf{k}_2$, $\mathbf{k}_1+\mathbf{k}_2+\mathbf{q}$, and $\mathbf{q}$ for the electron-hole, electron-electron, and the vertical channel, respectively. The full vertex Γ in high dimensions reduces to a sum

$$\Gamma(\mathbf{k}_1,z_1,\mathbf{k}_2,z_2;\mathbf{q})=\Gamma^{eh}(\mathbf{k}_1-\mathbf{k}_2;z_1,z_2)+\Gamma^{ee}(\mathbf{k}_1+\mathbf{k}_2+\mathbf{q};z_1,z_2)+\Gamma^{v}(\mathbf{q};z_1,z_2)-2\gamma(z_1,z_2), \quad (24)$$

where we had to subtract appropriately the local vertex to avoid double counting. Note that the CPA vertex as derived by Velický[5] equals Γ^{eh} and does not correspond to the leading high-dimensional asymptotics of the exact two-particle vertex.

Representation (23) uses the natural high-dimensional separation of the diagonal and off-diagonal parts of the one-particle propagator. We can rewrite the asymptotic solution (23) to another form with full one-particle propagators, which is more appropriate for finite-dimensional systems. We denote a two-particle bubble

$$\chi^{\pm}(\mathbf{q};z_1,z_2)=\frac{1}{N}\sum_{\mathbf{k}} G(\mathbf{k},z_1)G(\mathbf{q}\pm\mathbf{k},z_2). \quad (25)$$

If we further use relation (15) we obtain a new representation for the two-particle vertex

$$\begin{aligned}\Gamma(\mathbf{k}_1,z_1,\mathbf{k}_2,z_2;\mathbf{q}) &= \Lambda(z_1,z_2)\left\{\frac{1}{1-\Lambda(z_1,z_2)\chi^{+}(\mathbf{k}_2-\mathbf{k}_1;z_1,z_2)}\right.\\ &-\frac{2}{1-\Lambda(z_1,z_2)G(z_1)G(z_2)}\\ &+\frac{\prod_{i=1}^{2}\dfrac{1-\Lambda(z_i,z_i)G(z_i)G(z_i)}{[1-\Lambda(z_i,z_i)\chi^{+}(\mathbf{q};z_i,z_i)]}}{1-\Lambda(z_1,z_2)G(z_1)G(z_2)}\\ &\left.+\frac{1}{1-\Lambda(z_1,z_2)\chi^{-}(\mathbf{k}_1+\mathbf{k}_2+\mathbf{q};z_1,z_2)}\right\}, \quad (26)\end{aligned}$$

where $\Lambda(z_1,z_2)$ is the CPA irreducible vertex.

Note that the asymptotic solution for the two-particle vertex can no longer be represented via a single Bethe-Salpeter equation. It is because we have three asymptotically equally important but topologically different contributions. Each of them is marked by a different fixed two-particle momentum.

III. WARD IDENTITIES AND THE SELF-ENERGY

In the preceding section we derived a closed set of parquet equations determining the irreducible two-particle vertex functions from the given propagators $G^{loc}(z)$ and $G(\mathbf{k},z)$. The former is the site-diagonal part of the CPA propagator but the latter has not yet been specified. It is determined by a self-energy $\Sigma(\mathbf{k},z)$ from the Dyson Eq. (5). We have not yet demanded any relation between the self-energy and the vertex functions. We, however, know that thermodynamic consistence demands that the irreducible one- and two-particle functions be not independent. They are related by the differential Ward identity (10). To turn the parquet equations into a conserving approximation we have to fulfill the Ward identity and relate the self-energy to the solution of the parquet equations. The functional differential identity (10) is of little practical help in calculating the self-energy from the irreducible two-particle functions. Fortunately there are integral forms of the Ward identity relating one- and two-particle averaged functions that can be used to determine the self-energy from a known two-particle irreducible vertex.

A first integral Ward identity was derived by Velický[5] in the framework of the coherent-potential approximation. It

holds quite generally beyond the CPA and reads in our notation

$$\sum_j G^{(2)}_{ij,jk}(z_1,z_2) = -\frac{1}{\Delta z}\Delta G_{ik}, \tag{27a}$$

where $\Delta z = z_1 - z_2$, $\Delta G_{ij} = G_{ij}(z_1) - G_{ij}(z_2)$. We show in the appendix that this identity is a consequence of completeness of the eigenstates of the Hamiltonian and hence of probability conservation. This identity can be rewritten in momentum space

$$\frac{1}{N}\sum_{\mathbf{q}} G^{(2)}(\mathbf{k},z_1,\mathbf{k},z_2;\mathbf{q}) = -\frac{1}{\Delta z}[G(\mathbf{k},z_1) - G(\mathbf{k},z_2)]. \tag{27b}$$

Ward identity (27) is inconvenient for application, since it connects one- and two-particle averaged functions. We better have a relation between irreducible one- and two-particle functions like Eq. (10). An integral form of such a Ward identity was proven diagrammatically by Vollhardt and Wölfle[27] and reads

$$\Sigma(\mathbf{k}_1,z_1) - \Sigma(\mathbf{k}_2,z_2) = \frac{1}{N}\sum_{\mathbf{q}} \Lambda^{eh}(\mathbf{k}_1,z_1,\mathbf{k}_2,z_2;\mathbf{q}) \times [G(\mathbf{k}_1+\mathbf{q},z_1) - G(\mathbf{k}_2+\mathbf{q},z_2)]. \tag{28}$$

The diagrammatic derivation of the Vollhardt-Wölfle identity (28) utilizes a symmetry of the Anderson disordered model but does not establish a direct relation to conservation laws as the derivation of the Velický identity (27). We show in the appendix that the Vollhardt-Wölfle identity with $\mathbf{k}_1 = \mathbf{k}_2$ follows directly from Eq. (27) and the Bethe-Salpeter equation. At least this simplified form of the Vollhardt-Wölfle identity can be shown to be a consequence of probability conservation.[28]

To complete the parquet approximation for the two-particle irreducible vertex functions we can use Eq. (28) for $\mathbf{k}_1 = \mathbf{k}_2$ the boundary values of the complex energies along the real axis. We chose $z_1 = \omega_+$ and $z_2 = \omega_-$ where $\omega_\pm = \omega \pm i\eta$ and $\eta \searrow 0$. We obtain a relation

$$\mathrm{Im}\,\Sigma(\mathbf{k},\omega_+) = \frac{1}{N}\sum_{\mathbf{k}'} \Lambda^{eh}(\mathbf{k},\omega_+,\mathbf{k},\omega_-;\mathbf{k}-\mathbf{k}')\,\mathrm{Im}\,G(\mathbf{k}',\omega_+), \tag{29a}$$

determining the imaginary part of the self-energy along the real axis from the known irreducible vertex in the electron-hole channel. A similar formula can be derived for the irreducible vertex from the electron-electron channel, cf. the appendix.

Next we rely on analytic properties of the self-energy in the upper and lower complex half-planes and determine its real part along the real axis from the Kramers-Kronig relation

$$\mathrm{Re}\,\Sigma(\mathbf{k},\omega_+) = P\int_{-\infty}^{\infty}\frac{d\omega'}{\pi}\frac{\mathrm{Im}\,\Sigma(\mathbf{k},\omega'_+)}{\omega'-\omega}. \tag{29b}$$

The self-energy from the cut along the real axis can be analytically continued to energies in the upper and lower complex half-planes. The one-particle perturbed propagator from the parquet Eqs. (20b) can now be defined from the irreducible vertex via

$$\tilde{G}(\mathbf{k},\omega_+) = [\omega_+ - \epsilon(\mathbf{k}) - \Sigma(\mathbf{k},\omega_+)]^{-1} - G^{loc}(\omega_+) \tag{30}$$

with the self-energy from Eq. (29) and the local propagator from Eq. (12).

Equations (29) and (30) complete the parquet approach to disordered systems and make it a consistent and conserving scheme approximating simultaneously both the one- and two-particle irreducible functions. Neither the Bethe-Salpeter Eqs. (20b) nor Eqs. (29) violate analytic properties, unless there is a transition to another phase such as Anderson localization. The analyticity of the parquet approximation in the diffusive regime is then completely determined by its input, the two-particle local CPA vertex $\gamma(z_1,z_2)$ that is known to possess Herglotz analyticity.[29]

The advantage of the parquet approach to disordered systems is that we do not need to bother about the diagrams contributing to the self-energy to obtain a consistent approximation with the proper analytic behavior of the averaged Green functions.[30] An explicit sufficient condition for analyticity of a solution of the parquet approximation from Eq. (29a) is

$$\Lambda^{eh}(\mathbf{k},\omega_+,\mathbf{k},\omega_-;\mathbf{q}) \geqslant 0. \tag{31}$$

It can be checked in each step of iterations toward the full solution of the parquet approximation for the one- and two-particle irreducible functions.

IV. ELECTRICAL CONDUCTIVITY

The CPA constitutes a rather good approximation for the one-particle self-energy but completely fails to incorporate coherence in the propagation of pairs of particles. The emphasis in the parquet approach is hence laid on a systematic construction of diagrammatic approximations for nonlocal two-particle functions, in particular those determining transport properties and reflecting Anderson localization. In this section we show how a solution of the parquet approximation can be used in the calculation of the electrical conductivity.

We use a Kubo formula for the electrical conductivity with the current-current correlation function. If $\sigma_{\alpha\beta}$ is the complex conductivity and $\Pi_{\alpha\beta}$ the current-current correlation function we can write[31]

$$\sigma_{\alpha\beta}(\mathbf{q},E_+) = \frac{i}{E}\Pi_{\alpha\beta}(\mathbf{q},E_+), \tag{32}$$

where again $E_+ = E + i0^+$. The current-current correlation function can be expressed via a Kubo formula with the full two-particle vertex Γ,

$$\Pi_{\alpha\beta}(\mathbf{q},i\nu_m)=\frac{e^2}{4m^2}\frac{1}{N^2}\sum_{\mathbf{k},\mathbf{k}'}[\partial_\alpha(\epsilon(\mathbf{k}+\mathbf{q})-\epsilon(-\mathbf{k}))\times\partial_\beta(\epsilon(\mathbf{k}'+\mathbf{q})-\epsilon(-\mathbf{k}'))]k_BT\times\sum_{n=-\infty}^{\infty}\{G(\mathbf{k},i\omega_n)G(\mathbf{k}+\mathbf{q},i\omega_n+i\nu_m)\times[\delta(\mathbf{k}-\mathbf{k}')+\Gamma(\mathbf{k},i\omega_n,\mathbf{k}+\mathbf{q},i(\omega_n+\nu_m);\mathbf{k}'-\mathbf{k})\times G(\mathbf{k}',i\omega_n)G(\mathbf{k}'+\mathbf{q},i\omega_n+i\nu_m)]\}. \quad (33)$$

Here $\omega_n=(2n+1)\pi T$ and $\nu_m=2m\pi T$ are Matsubara frequencies.

We are actually interested only in the real part of the complex conductivity for real energies. We can then analytically continue the expression on the right-hand side of Eq. (33). For the real part of the conductivity we obtain

$$\begin{aligned}\mathrm{Re}\,\sigma_{\alpha\beta}(\mathbf{q},E)&=-\frac{e^2}{4}\frac{1}{N^2}\sum_{\mathbf{k},\mathbf{k}'}(v_\alpha(\mathbf{k}+\mathbf{q})+v_\alpha(\mathbf{k}))(v_\alpha(\mathbf{k}'+\mathbf{q})+v_\beta(\mathbf{k}'))\\&\times\frac{1}{2i}\sum_\sigma\sigma\frac{1}{2i}\sum_\tau\tau\int_{-\infty}^{\infty}\frac{d\omega}{\pi}\frac{f(\omega+E)-f(\omega)}{E}\\&\times\{G(\mathbf{k},\omega+i\sigma0^+)G(\mathbf{k}+\mathbf{q},\omega+E+i\tau0^+)\\&\times[\delta(\mathbf{k}-\mathbf{k}')+\Gamma(\mathbf{k},\omega+i\sigma0^+,\\&\mathbf{k}+\mathbf{q},\omega+E+i\tau0^+;\mathbf{k}'-\mathbf{k})\\&\times G(\mathbf{k}',\omega+i\sigma0^+)G(\mathbf{k}',\omega+i\tau0^+)]\},\end{aligned} \quad (34)$$

where $f(E)$ is the Fermi function and we denoted the group velocity $v_\alpha(\mathbf{k})=m^{-1}\partial\epsilon(\mathbf{k})/\partial k_\alpha$ and $\sigma,\tau=\pm1$. In most situations the static optical conductivity $(\mathbf{q}=0,E=0)$ at zero temperature is of interest. Expression (34) reduces in this case to

$$\begin{aligned}\mathrm{Re}\,\sigma_{\alpha\beta}=\frac{e^2}{4\pi}\frac{1}{N^2}\sum_{\mathbf{k},\mathbf{k}'}v_\alpha(\mathbf{k})v_\beta(\mathbf{k}')\sum_{\sigma\tau}(-\sigma\tau)\\\times G(\mathbf{k},E_F+i\sigma0^+)G(\mathbf{k},E_F+i\tau0^+)[\delta(\mathbf{k}-\mathbf{k}')\\+\Gamma(\mathbf{k},E_F+i\sigma0^+,\mathbf{k},E_F+i\tau0^+;\mathbf{k}'-\mathbf{k})\\\times G(\mathbf{k}',E_F+i\sigma0^+)G(\mathbf{k}',E_F+i\tau0^+)].\end{aligned} \quad (35)$$

We immediately see that the vertex function Γ contributes to the conductivity only if it depends on the transfer momentum $\mathbf{k}'-\mathbf{k}$. It is due to the symmetry $\epsilon(\mathbf{k})=\epsilon(-\mathbf{k})$ and $v_\alpha(\mathbf{k})=-v_\alpha(-\mathbf{k})$. Since the CPA vertex does not depend on the transfer momentum, the vertex corrections to the single-bubble electrical conductivity vanish in the CPA treatment.

Equation (35) is not appropriate for approximate calculations of the electrical conductivity. The vertex corrections contained in Γ are *added* to the single-bubble conductivity so that their negative contributions may reverse the positive sign of the conductivity, thus leading to unphysical behavior.

To avoid such a situation we represent the conductivity in a different way.[20] We utilize the Bethe-Salpeter equation in the electron-hole channel to represent the vertex Γ via the irreducible one, Λ^{eh}. Inserting its formal solution into Eq. (35) we obtain a new, equivalent representation for the conductivity

$$\mathrm{Re}\,\sigma_{\alpha\beta}=\frac{e^2}{4\pi}N^2\sum_{\mathbf{k},\mathbf{k}'}v_\alpha(\mathbf{k})v_\beta(\mathbf{k}')\sum_{\sigma\tau}(-\sigma\tau)G_\sigma(\mathbf{k})G_\tau(\mathbf{k})\times\{1-[\Lambda^{eh}_{\sigma\tau}G_\sigma G_\tau\bullet\}^{-1}(\mathbf{k},\mathbf{k};\mathbf{k}'-\mathbf{k}), \quad (36)$$

where we denoted $G_\sigma(\mathbf{k})=G(\mathbf{k},E_F+i\sigma0^+)$ and $\Lambda^{eh}_{\sigma\tau}=\Lambda^{eh}(\mathbf{k},E_F+i\sigma0^+,\mathbf{k}',E_F+i\tau0^+;\mathbf{q})$. At least for not too strong disorder, the norm of the operator $\|\Lambda^{eh}_{\sigma\tau}G_\sigma G_\tau\|\lesssim1$. Hence the conductivity remains in this representation nonnegative and free of spurious unphysical behavior. However, unlike formula (35), representation (36) is implicit and its application is conditioned by our ability to solve the Bethe-Salpeter integral equation in the electron-hole channel explicitly.

A. Asymptotic expression in high dimensions

To be explicit in the assessment of the contributions of the two-particle vertex to the electrical conductivity we again resort to the limit of high spatial dimensions where we know the vertex and the self-energy explicitly. We use a hypercubic lattice with a dispersion relation $\epsilon(\mathbf{k})=-t/(2d)^{1/2}\Sigma_{\nu=1}^{d}\cos k_\nu$, where the group velocity is $v_\alpha(\mathbf{k})=t/(2d)^{1/2}\sin k_\alpha$. Further on we use an analytic representation for the two-particle bubble in high dimensions where it can be represented via a double Gaussian integral[32]

$$\begin{aligned}\chi^{\pm}(\mathbf{q};z_1,z_2)=-\,\mathrm{sgn}(\mathrm{Im}\,z_1\mathrm{Im}\,z_2)\\\times\int_{-\infty}^{\infty}d\lambda_1d\lambda_2\theta(\lambda_1\mathrm{Im}\,z_1)\theta(\lambda_2\mathrm{Im}\,z_2)\\\times\exp\{i[\lambda_1x(z_1)+\lambda_2x(z_2)]\\-\tfrac{1}{4}[\lambda_1^2+\lambda_2^2+2\lambda_1\lambda_2X(\mathbf{q})]\},\end{aligned} \quad (37)$$

with $x(z)=z-\Sigma(z)$, $X(\mathbf{q})=1/d\Sigma_{\nu=1}^{d}\cos(q_\nu)$, and the Heaviside step function is $\theta(x)$. Only parallel conductivity survives on a hypercubic lattice and the integrals over the Brillouin zone of squares of the velocity factorize, i.e.,

$$\sum_{\mathbf{k}}v_\alpha(\mathbf{k})^2G_\sigma(\mathbf{k})G_\tau(\mathbf{k}+\mathbf{q})=\frac{t^2}{2d}\chi_{\sigma\tau}(\mathbf{q}). \quad (38)$$

Using the above representations and simplifications in Eqs. (26) and (35) we obtain after straightforward manipulations an explicit asymptotic formula for the conductivity in high spatial dimensions,

$$\frac{\pi}{e^2}\mathrm{Re}\,\sigma_{\alpha\alpha}=\frac{t^2}{2d}\langle|\mathrm{Im}\,G_+|^2\rangle-\frac{t^4}{16d^2}\mathrm{Re}\Bigg\{\frac{\langle G_+^2\rangle^4}{G_+^4}\times\Bigg[\Bigg\langle\frac{1}{(1+G_+(\Sigma_+-V_i))^2}\Bigg\rangle_{av}-1\Bigg]^2+\frac{\langle|G_+|^2\rangle^2}{|G_+|^2}\Bigg[\Bigg\langle\frac{1}{|1+G_+(\Sigma_+-V_i)|^2}\Bigg\rangle_{av}-1\Bigg]\times\Bigg(\frac{|\langle G_+^2\rangle|^2}{|G_+|^2}\Bigg[\Bigg\langle\frac{1}{|1+G_+(\Sigma_+-V_i)|^2}\Bigg\rangle_{av}-1\Bigg]-2\frac{\langle G_+^2\rangle^2}{G_+^2}\Bigg[\Bigg\langle\frac{1}{(1+G_+(\Sigma_+-V_i))^2}\Bigg\rangle_{av}-1\Bigg]\Bigg)\Bigg\},\tag{39}$$

where we used abbreviations $\langle G_+\rangle=N^{-1}\Sigma_{\mathbf{k}}G(\mathbf{k},E_F+i0^+)$, $\langle G_+^2\rangle=N^{-1}\Sigma_{\mathbf{k}}G(\mathbf{k},E_F+i0^+)^2$, and $\Sigma_+=\Sigma(E_F+i0^+)$. The one-particle propagators are the CPA ones calculated with the self-energy from the local approximation (12). Conductivity (39) depends explicitly only on the disorder distribution and the dimensionality. The vertex contribution, proportional to t^4/d^2, has a negative sign and we cannot guarantee positivity of the conductivity. Although the vertex corrections are negligible in the limit $d\to\infty$ they may turn the overall sign of the conductivity negative for a fixed finite dimension d. Whether conductivity (39) for a fixed dimension is positive or negative depends on the band filling and the disorder distribution and strength. Vanishing of the asymptotic conductivity in this representation does not indicate Anderson localization but merely a limit upon the dimension below which formula (39) cannot be applied.

B. Mean-field expression for vertex corrections to the electrical conductivity

The limit of high spatial dimensions is usually used in order to set a mean-field approximation for a physical quantity. We showed in the preceding subsection that the vertex corrections are asymptotically less important than the one-electron, single-bubble term. But the vertex corrections may, in finite dimensions, turn static optical conductivity negative. Expression (35) with the asymptotic solution for the vertex function in high dimensions is hence unsuitable for serving as a mean-field approximation, since physical consistence of the result is not guaranteed. We can take the leading single-bubble term as a mean-field approximation for the conductivity as is actually common in the literature. Or, when we are interested in the impact of vertex corrections, we have to use representation (36) and evaluate its leading asymptotic behavior in high spatial dimensions as suggested recently.[20]

The limit of high spatial dimensions enables one to solve the Bethe-Salpeter equation in the electron-hole channel explicitly. We need only its leading asymptotic order. Note that only the nonlocal part of the vertex $\Lambda^{eh}(\mathbf{k},\mathbf{k};\mathbf{k}'-\mathbf{k})$ having odd parity with respect to reflections in $\mathbf{k}$ and $\mathbf{k}'$ contributes to the conductivity. We hence have to take its leading asymptotics into account. We derive it if we solve the Bethe-Salpeter equation in the electron-hole channel for Λ^{eh} instead for Γ, i.e., $\Lambda^{eh}=\Gamma\{\bullet[GG\Gamma]+1\}^{-1}$. Using vertex Γ from Eq. (24) one finds in the order $O(1/d)$

$$\Lambda^{eh}(\mathbf{k}_1,z_1,\mathbf{k}_2,z_2;\mathbf{q})=\Lambda(z_1,z_2)+(1-\Lambda(z_1,z_2)G(z_1)G(z_2))^2\times[\Gamma(\mathbf{k}_1,z_1,\mathbf{k}_2,z_2;\mathbf{q})-\Gamma^{eh}(\mathbf{k}_2-\mathbf{k}_1;z_1,z_2)].\tag{40}$$

In the limit $d\to\infty$ the momentum convolutions decouple. To derive the leading asymptotic contribution from the nonlocal part of Λ^{eh} to the conductivity we have to calculate the momentum convolutions at the level of order $O(1/d)$ so that the velocities appear in squares and the momentum integrals do not vanish. Keeping only the leading-order terms in the expansion of the denominator in Eq. (36) we end up with a mean-field-like expression for the dc conductivity[20]

$$\mathrm{Re}\,\sigma_{\alpha\alpha}=\frac{e^2}{4\pi}\sum_{\sigma\tau}(-\sigma\tau)\frac{\langle v_\alpha^2G_\sigma G_\tau\rangle}{1-\langle v_\alpha^2G_\sigma G_\tau\rangle\langle\Lambda'^{\alpha}_{\sigma\tau}\rangle},\tag{41a}$$

where $\langle v_\alpha^2G_\sigma G_\tau\rangle=N^{-1}\Sigma_{\mathbf{k}}v_\alpha(\mathbf{k})^2G_\sigma(\mathbf{k})G_\tau(\mathbf{k})$ and

$$\langle\Lambda'^{\alpha}_{\sigma\tau}\rangle=\frac{1}{N^2}\sum_{\mathbf{k},\mathbf{k}'}\frac{\delta^2}{\delta v_\alpha(\mathbf{k})\,\delta v_\alpha(\mathbf{k}')}\Lambda^{eh}_{\sigma\tau}(\mathbf{k},\mathbf{k};\mathbf{k}'-\mathbf{k}).\tag{41b}$$

The irreducible vertex Λ^{eh} is taken from Eq. (40). The one-particle propagators are those from the local, coherent-potential approximation, since it is the local irreducible vertex Λ that determines the leading high-dimensional asymptotics of the self-energy in Eq. (29a). However, only terms with odd symmetry with respect to time inversion contribute to the vertex corrections to the conductivity and we have to go to the leading order of the nonlocal part of Λ^{eh} to substantiate them. If one resorts to the local vertex Λ in Eq. (41) one recovers the CPA conductivity of the single electron-hole bubble.

Conductivity (41) with the CPA one-particle propagator can be called a mean-field approximation for the conductivity with vertex corrections, since the vertex corrections are determined from the asymptotic limit of high spatial dimensions. It can be applied in finite dimensions for $d>2$ with the appropriate lattice structure determined by the Brillouin zone. Note that the vertex Λ^{eh} from Eq. (40) contains a diffusion pole from the electron-electron channel and the integral in Eq. (41b) diverges in $d\leqslant 2$. Hence the mean-field description of vertex corrections breaks down there. In these low dimensions, where Anderson localization is expected, we have to use the full two-particle self-consistent parquet approximation in order to take properly into account the influence of the diffusion pole.

V. MEAN-FIELD VERTEX CORRECTIONS IN A BINARY ALLOY

A. High-dimensional approximation

Mean-field expression for the conductivity with vertex corrections (41) demands the evaluation of momentum integrals over the Brillouin zone to determine the averaged velocity and the derivative of the vertex Λ^{eh}. This must be done numerically for each particular lattice. To assess qualitatively the influence of the mean-field vertex corrections on the conductivity and to demonstrate physical consistency of approximation (41), i.e., overall non-negativity of the conductivity, we further simplify expression (41). We approximate the momentum integrals by their high-dimensional asymptotics, i.e., we replace the momentum integrals by integrals with the density of states. We use the same steps as in Sec. II C when deriving the high-dimensional asymptotics of the conductivity. Using vertex (40) we straightforwardly derive

$$\mathrm{Re}\,\sigma_{\alpha\alpha}=\left(\frac{e^2t^2}{8\pi d}\right)\sum_{\sigma\tau}\frac{(-\sigma\tau)\langle G_\sigma G_\tau\rangle}{1+\frac{t^2}{2d}\langle G_\sigma G_\tau\rangle\Lambda_{\sigma\tau}(1-\Lambda_{\sigma\tau}G_\sigma G_\tau)[\,\gamma_{\sigma\tau}\langle G_\sigma^2\rangle\langle G_\tau^2\rangle-\gamma_{\sigma\sigma}\langle G_\sigma^2\rangle^2-\gamma_{\tau\tau}\langle G_\tau^2\rangle^2]}, \tag{42}$$

where $\langle G_\sigma G_\tau\rangle$ is defined as in Eq. (39). The vertices Λ and γ are calculated in the local approximation from Sec. II A. We can explicitly sum over the indices σ,τ and obtain

$$\mathrm{Re}\,\sigma_{\alpha\alpha}=\left(\frac{e^2t^2}{4\pi d}\right)\left\{\frac{\langle|G_+|^2\rangle}{1+\frac{t^2}{2d}\langle|G_+|^2\rangle\Lambda_{+-}(1-\Lambda_{+-}|G_+|^2)[\,\gamma_{+-}|\langle G_\sigma^2\rangle|^2-2\,\mathrm{Re}(\,\gamma_{++}\langle G_+^2\rangle^2)]}-\mathrm{Re}\,\frac{\langle G_+^2\rangle}{1-\frac{t^2}{2d}\langle G_+^2\rangle^3\Lambda_{++}^2}\right\}. \tag{43}$$

For the explicit numerical calculations we choose a binary alloy with the site-diagonal disorder distribution

$$\rho(V)=x\,\delta(V-\Delta)+(1-x)\,\delta(V+\Delta). \tag{44}$$

To simplify the relation between the one- and two-particle functions we further choose a model density of states of a $d=\infty$ Bethe instead of a hypercubic lattice. It is characterized by an equation

$$G(z)=\frac{1}{z-G(z)}, \tag{45}$$

where we set the hopping $t=1$ with the energy band $E\in(-2,2)$. The self-energy for complex energies in this model is then determined from a cubic equation

$$0=G(z)^3-2zG(z)^2+(1-\Delta^2+z^2)G(z)-(z-(1-2x)\Delta) \tag{46a}$$

with

$$\Sigma(z)=z-G(z)-G(z)^{-1}. \tag{46b}$$

We resort to real frequencies $E_\sigma=E+i\sigma 0^+$ and take advantage of explicit representations of two-particle functions via one-particle local propagators

$$\langle G_\sigma G_\tau\rangle=\frac{G_\sigma G_\tau}{1-G_\sigma G_\tau} \tag{47}$$

and

$$\Lambda_{\sigma\tau}=\frac{1}{G_\sigma G_\tau}-\frac{1}{\frac{x}{(E-G_\sigma-\Delta)(E-G_\tau-\Delta)}+\frac{1-x}{(E-G_\sigma+\Delta)(E-G_\tau+\Delta)}}. \tag{48}$$

We use the above formulas together with a numerical solution to the self-energy from Eq. (46) in Eq. (43) to reach quantitative results for the electrical conductivity. In particular we are interested in the impact of vertex corrections onto the CPA conductivity. We set the formal parameter of the lattice dimension $d=3$ in Eq. (43). Figure 1 shows the CPA and the mean-field conductivity with vertex corrections as a function of energy for a fixed concentration $x=0.5$ and two values of the variance of the random potential (disorder strength). We see that the vertex corrections in general lower the single-bubble conductivity and hence the electron-electron multiple scatterings dominate. There are, however, situations where the vertex corrections due to electron-electron and hole-hole multiple scatterings may dominate

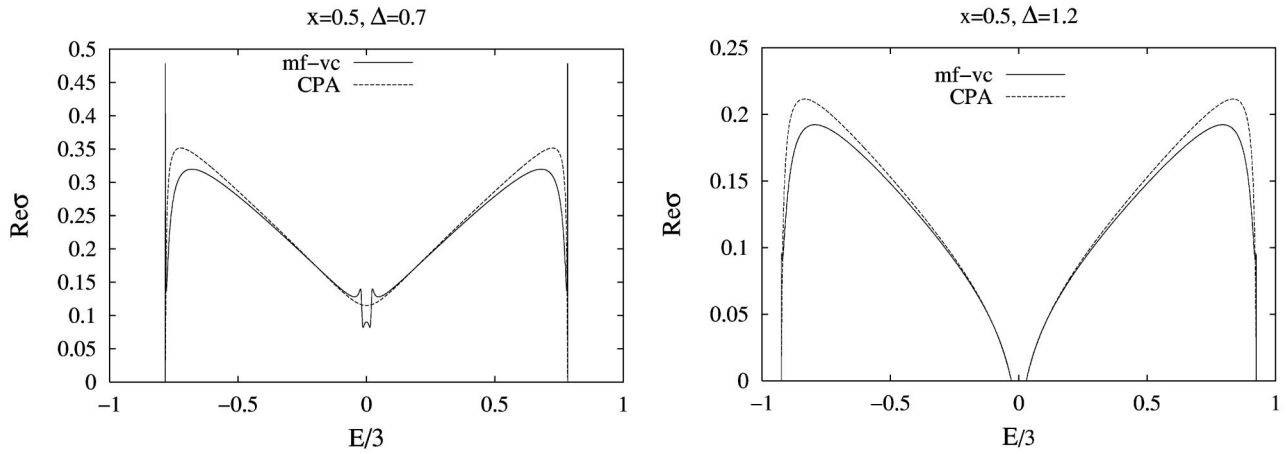

FIG. 1. Real part of the static conductivity as a function of energy for concentration $x=0.5$ and two values of disorder strength $\Delta=0.7$ and $\Delta=1.2$.

over the electron-hole crossed diagrams and cause an increase in the CPA conductivity. It happens in the proximity of nonanalyticities in the local CPA vertex. The real part of Λ_{++} for $\Delta=1/\sqrt{2}$ goes through zero and displays a pole for $x=0.5$. This singular behavior causes sharp mobility peaks at the band edges and irregularities near half-filling, $E=0$. Such a behavior is observed only for $\Delta\approx 1/\sqrt{2}$ and $x\approx 0.5$. Figure 2 shows the same for an asymmetric concentration $x=0.3$. The mobility edges are now less pronounced and the conductivity fluctuations inside the energy band are no longer symmetric.

Due to the structureless density of states of the Bethe lattice in $d=\infty$, vertex corrections do not alter the CPA conductivity significantly apart from the special situations influenced by the singularity in the CPA vertex Λ_{++}. Figure 3 shows the conductivity for the half-filled band as a function of concentration x. There is almost no significant difference between the conductivity with and without vertex corrections, except for concentrations $x\approx 0.5$.[33] An analogous picture is obtained for the conductivity as a function of the disorder strength Δ, where the differences are significant only around $\Delta\approx 1/\sqrt{2}$, Fig. 4.

B. Applicability of mean-field approximations in realistic calculations

Calculations in the preceding subsection served two purposes. First, we demonstrated how to reduce numerically the demanding expression (41) to a typical mean-field formula using only integrals over the density of states. Second, we justified application of the mean-field expression for the electrical conductivity with vertex corrections as a first step beyond the CPA conductivity. However, a natural question arises about applicability and reliability of mean-field expressions in realistic calculations of transport properties of alloys and relevance of vertex corrections (beyond CPA) there.

As we already discussed, mean-field expression for the conductivity with vertex corrections (41) is inapplicable in dimensions $d\leqslant 2$ due to the presence of a nonintegrable Cooperon pole at $\mathbf{k}+\mathbf{k}'=0$ in the vertex $\Lambda^{eh}(\mathbf{k},\mathbf{k}',\mathbf{q})$ from Eq. (40). In three dimensions this singularity is integrable and mean-field theory can, in principle, deliver good numerical results. A mean-field theory is reliable if the contribution to the conductivity from small momenta around the critical value $\mathbf{k}+\mathbf{k}'=0$ of the Cooperon pole does not dominate.

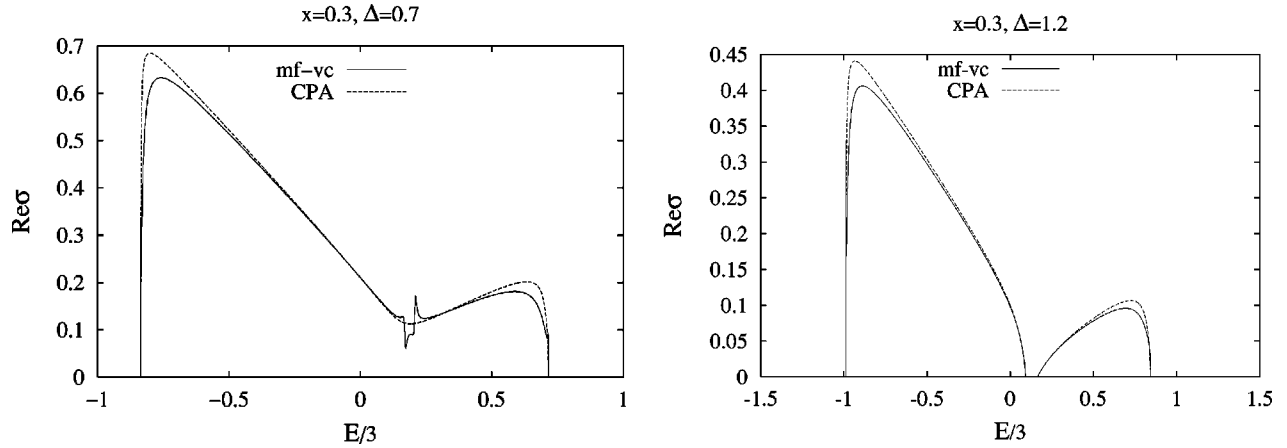

FIG. 2. Real part of the static conductivity as a function of energy for concentration $x=0.3$ and two values of disorder strength $\Delta=0.7$ and $\Delta=1.2$.

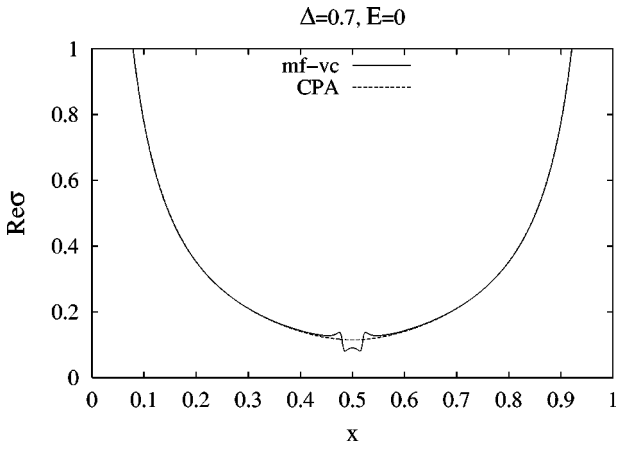

FIG. 3. Real part of the static conductivity as a function of concentration for the half-filled band and $\Delta = 0.7$.

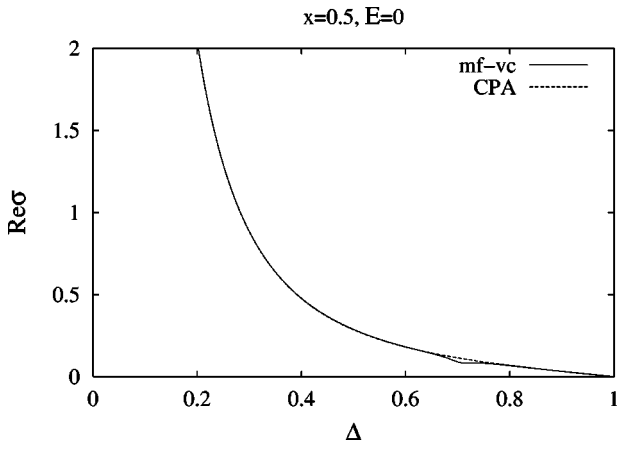

FIG. 4. Real part of the static conductivity as a function of disorder strength for the half-filled band and $x = 0.5$.

This cannot be decided from the mean-field theory itself but from small-momentum or long-distance approximations factorizing the singular (nonanalytic) contribution to the vertex function. Approximations with a long-range spatial coherence differ from mean-field, local theories where no preference in momenta is present and the spatial coherence is absent. To check applicability of the mean-field approximation in our approach we can use a small-momentum expansion for the bubble function $\chi^{\pm}(\mathbf{q};\omega+i0^{+},\omega+i0^{-})$, defined in Eq. (25), in the representation of the vertex Λ^{eh}, Eq. (40). If the leading order of the small-momentum expansion produces the conductivity of the order of the mean-field formula, then the mean-field approximation is qualitatively, and to a certain extent also quantitatively, reliable.

If we know or expect that the effect of the Cooperon pole is not critical for the static conductivity we can apply Eq. (41) to assess quantitatively the role of the vertex corrections. However, the evaluation of Eq. (41b) is numerically very demanding in $d=3$. It is meaningful to use explicit momentum integrals only if we expect strongly nonuniform behavior of the integrand in the first Brillouin zone. When the weight of the pole in the vertex functions is small, it is expedient to reduce the numerical expense. We use the simplification justified by the asymptotic limit of high lattice dimensions and replace the momentum integrals with energy ones as in the preceding subsection. Formula (43) can be generalized to a typical mean-field form

$$\mathrm{Re}\,\sigma_{\alpha\beta} = \left(\frac{e^2}{2\pi}\right)\left\{\frac{\langle v_\alpha v_\beta |G_+|^2\rangle}{1+\langle v_\alpha v_\beta |G_+|^2\rangle\Lambda_{+-}(1-\Lambda_{+-}|G_+|^2)[\gamma_{+-}|\langle G_\sigma^2\rangle|^2 - 2\,\mathrm{Re}(\gamma_{++}\langle G_+^2\rangle^2)]} - \mathrm{Re}\frac{\langle v_\alpha v_\beta G_+^2\rangle}{1-\langle v_\alpha v_\beta G_+^2\rangle\Lambda_{++}^2\langle G_+^2\rangle^2}\right\}, \tag{49}$$

where the lattice structure comes only via the density of states. This formula, completely disregarding the existence of the diffusion and Cooperon poles, can be formally applied in any lattice dimension.

In calculations of transport properties of alloys we have to use more realistic electron models with orbital degrees of freedom explicitly taken into account. This leads to a multiorbital situation to which the above expression is readily generalizable. Each quantity is replaced by a matrix with orbital indices and the multiplication is replaced by an appropriate matrix one. The multiorbital generalization of Eq. (49) is not the only source of mean-field vertex corrections in realistic calculations. The multiorbital CPA also produces vertex corrections as explicitly demonstrated in the framework of the Korringa-Kohn-Rostoker CPA by Butler.[34] We hence have to add to a multiorbital generalization of Eq. (49) a contribution from terms with odd symmetry with respect to the time inversion absent in the one-orbital case. Following Ref. 34 we can represent the odd part of the conductivity as

$$\mathrm{Re}\,\sigma_{\alpha\beta}^{odd} = \frac{e^2}{4\pi}\sum_{\sigma\tau}(-\sigma\tau)\sum_{LL'}\sum_{MM'}\langle \hat{v}_\alpha \hat{G}_\sigma \hat{G}_\tau\rangle_{LL'}[\hat{\chi}_{\sigma\tau}^{+}(0) \times\{1-\hat{\Lambda}_{\sigma\tau}\hat{\chi}_{\sigma\tau}^{+}(0)\}^{-1}]_{L'M'}\langle \hat{v}_\beta \hat{G}_\sigma \hat{G}_\tau\rangle_{M'M}, \tag{50}$$

where L,M are appropriate orbital indices. The CPA vertices, propagators, the bubble function χ, and the velocity $\mathbf{v}$ are now matrices in the orbital indices. Here we used the fact that only the vertex Γ^{eh} from the electron-hole channel con-

tributes in the mean-field limit. Note that only the off-diagonal elements of the velocity matrix can contribute to the conductivity, since the two velocities (electrical currents) in the Kubo formula are not spatially correlated.

The two parts of the mean-field conductivity Eqs. (49) and (50) enable us to analyze the role of the vertex corrections. As found earlier in the literature[34,35] the CPA vertex corrections Eq. (50) generally increase the single-bubble conductivity. It is due to the fact that the CPA vertex function Γ^{eh} from Eq. (23a) contains only direct electron-hole multiple scatterings that generally amplify the diffusion. The even part of the mean-field conductivity Eq. (49) is more complex. It contains contributions from multiple scattering from the electron-electron and the vertical channels. The former represent crossed scatterings in the vertex function or coherent backscatterings that hinder the electron propagation. They generate the positive term in the denominator on the right-hand side of Eq. (49). The scatterings from the vertical channel produce negative corrections in the denominator of Eq. (49) and increase the CPA conductivity. It is hence clear that conductivity Eq. (49) has a richer structure than the CPA odd term Eq. (50) and can either increase or decrease the one-particle conductivity depending on the values of the CPA local vertex functions.

Both contributions to the mean-field conductivity Eqs. (49) and (50) are of the same order of magnitude and comparably elaborate in the numerical evaluation. Since they completely disregard the singular behavior of the vertex function at $\mathbf{k}+\mathbf{k}'=0$ one cannot expect that the vertex corrections calculated from this mean-field approximation will produce drastic changes in the one-particle or semiclassical Boltzmann conductivity. This is even true in low dimensions in $d=1,2$. The low-dimensional calculations[34] serve only illustrative purposes and have no physical significance, since the mean-field description breaks down there. Mean-field approximations can efficiently be applied to the bulk conductivity of alloys, but only the sum of the even and odd contributions Eq. (49) and Eq. (50) can at least qualitatively estimate the trend toward electron localization, if present.

VI. CONCLUSIONS

We have developed a diagrammatic theory for constructing systematic approximations to nonlocal two-particle vertex functions of noninteracting electrons moving in a random potential. The underlying idea of our approach is to treat separately diagonal, local and off-diagonal, nonlocal elements of the two-particle vertex. To this purpose we used the asymptotic limit of high spatial dimensions. In the strict $d=\infty$ limit only the local one-particle propagator is relevant and the solution contains only single-site scatterings and reduces to the coherent-potential approximation. Beyond this limit we utilized ambiguity in the definition of the two-particle irreducibility. We classified the nonlocal contributions to the two-particle vertex according to the type of the two-particle irreducibility to which they belong. Like many-body theories there are three topologically inequivalent irreducibility channels according to which pairs of propagators interconnect spatially distinct two-particle scatterings on the random potential. Representing the two-particle vertex via Bethe-Salpeter equations and irreducible vertices in each channel and utilizing the topological inequivalence of these representations we derived a closed set of coupled (parquet) equations for the irreducible vertices. The irreducible vertices from the parquet equations were used in an integral form of the Ward identity to determine the self-energy of the parquet solution. In this way we completed the parquet equations to an approximation consistently determining all one- and two-particle functions. The input to the parquet approximation are the local CPA one-particle propagator and the local two-particle vertex. Neither the form of the parquet equations nor the Ward identity may cause unphysical nonanalyticities in the solution. Solutions to the parquet approximation hence inherit the analytic properties of the CPA input and are free of spurious, unphysical behavior.

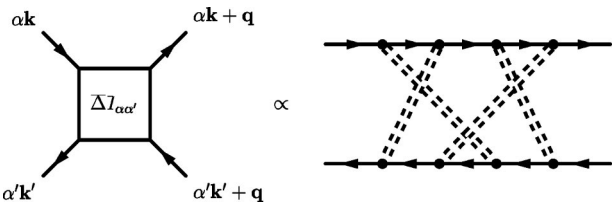

FIG. 5. Lowest-order correction to the completely two-particle irreducible vertex $I_{\alpha\alpha'}=\gamma_{\alpha\alpha'}$ from the parquet approximation. The double-dashed line is the CPA local vertex $\gamma_{\alpha\alpha'}$. The internal fermion lines stand for the CPA off-diagonal propagator G^{off}.

The proposed diagrammatic implementation of nonlocal corrections to the CPA aims primarily at improving the CPA two-particle functions on a long-range scale. Although there is no obvious small parameter controlling the nonlocal corrections to the CPA, systematic improvements of the local approximation are controlled via diagrams to the completely two-particle irreducible vertex I. In the parquet approximation the input is $I=\gamma$, the local vertex from Eq. (15). A first correction ΔI to the input of the parquet approximation is proportional to $\gamma^4(G^{off})^6$, where G^{off} is the off-diagonal element of the CPA propagator, see Fig. 5. It means that in the weak-disorder limit the parquet approximation is exact up to V^7 whereas CPA only to V^3 in powers of the random potential. The parquet approximation represents a significant systematic improvement of the CPA in the weak-disorder limit. We showed that beyond the weak-disorder limit the parquet approximation contains the exact asymptotics of the two-particle functions up to d^{-2}. This fact we used in proposing a mean-field approximation for the electrical conductivity with vertex corrections.

It is not, however, the weak-scattering limit where the assets of the parquet approach to disordered systems lie. The parquet approach is in particular appropriate for apprehending spatial quantum coherence and backscattering effects. The parquet approximation even in the first iteration (high-dimensional asymptotics) contains an infinite number of ''crossed'' two-particle diagrams. The weak localization with the Cooperon pole and a long-range spatial coherence from backscatterings are included. Most importantly, however, the parquet equations for the irreducible two-particle vertex functions are fully self-consistent. They can adequately deal

with poles and divergences in the vertex functions and can hence significantly change the diffusive character of the electronic transport in low dimensions and strong disorder.

We hope that the presented parquet approach can bridge the gap between the mean-field coherent-potential approximation on the one side and localization theories on the other side. Whether the parquet equations can actually describe the localization transition must be decided by solving the full set of self-consistent coupled integral equations for the vertex functions and the self-energy. This has been left for future research.

ACKNOWLEDGMENTS

It is my pleasure to acknowledge numerous stimulating and fruitful conversations with D. Vollhardt. I also benefited from discussions with B. Velický, J. Kudrnovský, V. Drchal, and V. Špička on various aspects of the electronic transport in random media. The work was supported in part by Grant Nos. 202/98/1290 and 202/01/0764 of the Grant Agency of the Czech Republic.

APPENDIX: ALGEBRAIC DERIVATION OF WARD IDENTITIES

We use algebraic identities to prove Eq. (27) and the special case of Eq. (28) with $\mathbf{k}_1=\mathbf{k}_2$.

The two-particle function can be defined as a matrix element of a tensor (direct) product $G^{(2)}_{ij,kl}(z_1,z_2)=\langle\langle ik|\hat{G}(z_1)\otimes\hat{G}(z_2)|jl\rangle\rangle_{av}$ where the resolvent operator is defined as $\hat{G}(z)=[z\hat{1}-\hat{t}-\hat{V}]^{-1}$ and the basis vectors are Wannier orbitals at the lattice sites. Using this lattice-space representation we define a ''projection'' onto the one-particle subspace by equaling the basis states from the left and right Hilbert space. When we sum over one set of indices ($k=j$) we reduce the direct product from the two-particle Hilbert space to an operator multiplication in the one-particle Hilbert space. Ward identity (27) is then a consequence of an operator identity

$$[z_1\hat{1}-\hat{H}]^{-1}\cdot[z_2\hat{1}-\hat{H}]^{-1}=[z_2-z_1]^{-1}\{[z_1\hat{1}-\hat{H}]^{-1}-[z_2\hat{1}-\hat{H}]^{-1}\}, \tag{A1}$$

where $\hat{H}=\hat{t}+\hat{V}$. Identity (A1) holds for each configuration of the random potential $\hat{V}$ and after its configurational averaging we obtain Eq. (27). Ward identity (27) is hence a consequence of *completeness* of the eigenstates of the Hamilton operator. Completeness of the eigenstates reflects *conservation of probability* and is a necessary prerequisite for conservation of energy and other physical quantities.

To prove the Ward identity (28) with $\mathbf{k}_1=\mathbf{k}_2$ we use the Bethe-Salpeter equation in the electron-hole channel

$$G^{(2)}_{ij,kl}(z_1,z_2)=G_{ij}(z_1)G_{kl}(z_2)+\sum_{i'j'k'l'}G_{ii'}(z_1)G_{ll'}(z_2)\times\Lambda^{eh}_{i'j',k'l'}(z_1,z_2)G^{(2)}_{j'j,kk'}(z_1,z_2). \tag{A2}$$

We multiply it with the inverse one-particle propagators from left and right and obtain

$$\sum_{i'l'}G^{-1}_{ii'}(z_1)G^{-1}_{ll'}(z_2)G^{(2)}_{i'j,kl'}(z_1,z_2)=\delta_{ij}\delta_{kl}+\sum_{j'k'}\Lambda^{eh}_{ij',k'l}(z_1,z_2)G^{(2)}_{j'j,kk'}(z_1,z_2). \tag{A3}$$

Summing over the intermediate indices and using Eq. (27) we find

$$\sum_{i'jl'}G^{-1}_{ii'}(z_1)G^{-1}_{ll'}(z_2)G^{(2)}_{i'j,jl'}(z_1,z_2)=\frac{1}{\Delta z}[G^{-1}_{il}(z_1)-G^{-1}_{il}(z_2)]. \tag{A4}$$

We insert Eqs. (A4) and (27) in Eq. (A3) and obtain the desired identity for the self-energy

$$\Delta\Sigma_{il}=\sum_{j'k'}\Lambda^{eh}_{ij',k'l}(z_1,z_2)\Delta G_{j'k'}. \tag{A5}$$

It reads in momentum space

$$\Sigma(\mathbf{k},z_1)-\Sigma(\mathbf{k},z_2)=\frac{1}{N}\sum_{\mathbf{k}'}\Lambda^{eh}(\mathbf{k},z_1,\mathbf{k},z_2;\mathbf{k}'-\mathbf{k})[G(\mathbf{k}',z_1)-G(\mathbf{k}',z_2)]. \tag{A6}$$

Analogously we can derive a Ward identity for the vertex function from the electron-electron channel

$$\Sigma(\mathbf{k},z_1)-\Sigma(-\mathbf{k},z_2)=\frac{1}{N}\sum_{\mathbf{k}'}\Lambda^{ee}(\mathbf{k},z_1,-\mathbf{k}',z_2;\mathbf{k}'-\mathbf{k})\times[G(\mathbf{k}',z_1)-G(-\mathbf{k}',z_2)]. \tag{A7}$$

*E-mail address: janis@fzu.cz

[1] P. Soven, Phys. Rev. **156**, 809 (1967).
[2] B. Velický, S. Kirkpatrick, and H. Ehrenreich, Phys. Rev. **175**, 745 (1968).
[3] R. J. Elliot, J. A. Krumhansl, and P. L. Leath, Rev. Mod. Phys. **46**, 465 (1974).
[4] I. Turek, V. Drchal, J. Kudrnovský, M. Šob, and P. Weinberger, *Electronic Structure of Disordered Alloys, Surfaces and Interfaces* (Kluwer, Boston, 1997).
[5] B. Velický, Phys. Rev. **184**, 614 (1969).
[6] P. A. Lee and R. V. Ramakrishnan, Rev. Mod. Phys. **57**, 287 (1985).
[7] H. Itoh, A. Shibata, T. Kumazaki, J. Inoue, and S. Maekawa, J. Phys. Soc. Jpn. **68**, 1632 (1999); P. Bruno, H. Itoh, J. Inoue, and S. Nonoyama, J. Magn. Magn. Mater. **198-9**, 46 (1999).
[8] A. Gonis, *Green Functions for Ordered and Disordered Systems*, edited by E. van Groessen and E. M. de Jager, Studies in Mathematical Physics (North-Holland, Amsterdam, 1992).

[9] R. Mills and P. Ratanavararaksa, Phys. Rev. B **18**, 5291 (1978).
[10] T. Kaplan, P. L. Leath, L. J. Gray, and H. W. Diehl, Phys. Rev. B **21**, 4230 (1980).
[11] V. Čápek, Phys. Status Solidi B **52**, 399 (1972).
[12] W. H. Butler and B. G. Nickel, Phys. Rev. Lett. **30**, 373 (1973).
[13] M. Jarrell and H. R. Krishnamurthy, cond-mat/0006431 (unpublished); Phys. Rev. B **63**, 125102 (2001).
[14] D. Vollhardt and P. Wölfle, in *Electronic Phase Transitions*, edited by W. Hanke and Yu. V. Kopaev (Elsevier, Amsterdam, 1992), p. 1.
[15] B. Kramer and A. MacKinnon, Rep. Prog. Phys. **56**, 1469 (1993).
[16] C. De Dominicis, J. Math. Phys. **3**, 983 (1962); *ibid.* **4**, 255 (1963); C. De Dominicis and P. C. Martin, *ibid.* **5**, 14 (1964); *ibid.* **5**, 31 (1964).
[17] A. D. Jackson, A. Lande, and R. A. Smith, Phys. Rep. **86**, 55 (1982).
[18] N. E. Bickers and S. R. White, Phys. Rev. B **43**, 8044 (1991); N. E. Bickers, Int. J. Mod. Phys. B **5**, 253 (1991).
[19] V. Janiš, Phys. Rev. B **60**, 11 345 (1999).
[20] For a review on the limit of high spatial dimensions see A. Georges, G. Kotliar, W. Krauth, and M. Rozenberg, Rev. Mod. Phys. **68**, 13 (1996). Systems with site-diagonal disorder within this approach were studied, e.g., in R. Vlaming and D. Vollhardt, Phys. Rev. B **45**, 4637 (1992); V. Janiš and D. Vollhardt, *ibid.* **46**, 15 712 (1992).
[21] V. Janiš, Phys. Rev. Lett. **83**, 2781 (1999).
[22] V. Janiš and D. Vollhardt, Phys. Rev. B **63**, 125102 (2001).
[23] Details of the diagrammatic techniques in disordered electron systems can be found in the original papers, S. F. Edwards, Philos. Mag. **3**, 1020 (1958); J. S. Langer, Phys. Rev. **120**, 714 (1960); and in Refs. 3, 14, and 15.
[24] G. Baym and L. P. Kadanoff, Phys. Rev. **124**, 287 (1961).
[25] A two-particle function is called completely irreducible if it is irreducible in all two-particle channels, i.e., it can be disconnected by cutting at least three lines (one-particle propagators).
[26] W. Metzner and D. Vollhardt, Phys. Rev. Lett. **62**, 324 (1989).
[27] D. Vollhardt and P. Wölfle, Phys. Rev. B **22**, 4666 (1980),
[28] We have not found any identity between one- and two-particle averaged Green functions that would lead to the most general form of identity (28) being a formal but straightforward result of a functional integration of the differential identity (10).
[29] E. Müller-Hartmann, Solid State Commun. **12**, 1269 (1973).
[30] Note that not all diagrammatic approximations for the vertex function with the self-energy calculated via the Ward identity (29) allow for a closed set of self-energy diagrams. We actually do not need this property for a physically consistent picture, since no physical law is broken. The Feynman diagrams serve to control the approximation made in the entire phase space. This is done in the parquet approach at the two-particle level. The self-energy calculated via the Ward identity is defined only at the saddle point and does not have a variational character as a diagrammatically derived one.
[31] G. D. Mahan, *Many-Particle Physics* (Plenum, New York, 1990), Sec. 3.8.
[32] E. Müller-Hartmann, Z. Phys. B: Condens. Matter **74**, 507 (1989); U. Brandt and C. Mielsch, *ibid.* **75**, 365 (1989).
[33] Rather insignificant differences in the mean-field conductivity with and without vertex corrections observed here are caused by the asymptotic limit $d\to\infty$. This limit is needed to keep global consistence between one-particle (CPA with local self-energy) and two-particle Green functions. When mean-field conductivity (41) is applied in three dimensions, the Ward identity (29) has to be used to adjust the self-energy. Even for the vertex function (40) the self-energy becomes nonlocal. The vertex corrections from Eq. (41) not only cause important changes in the conductivity but also in the band structure of finite-dimensional systems, in particular near band edges. In low dimensions, $d\leqslant 2$, the asymptotic expression for the irreducible vertex (40) becomes inapplicable due to diffusion and Cooperon poles and we have to leave the mean-field concept and solve the parquet Eqs. (19) with other means.
[34] W. H. Butler, Phys. Rev. B **31**, 3260 (1985).
[35] J. Banhart, H. Ebert, P. Weinberger, and J. Voitländer, Phys. Rev. B **50**, 2104 (1994); J. Banhart, Philos. Mag. B **77**, 85 (1998); *ibid.* **77**, 105 (1998).